

Published in final edited form as:

*Invest Radiol.* 2012 October ; 47(10): 588–595. doi:10.1097/RLI.0b013e318260abb3.

## Hepatic Blood Perfusion Estimated by Dynamic Contrast-Enhanced Computed Tomography in Pigs *Limitations of the Slope Method*

Michael Winterdahl, PhD<sup>1</sup>, Michael Sørensen, PhD<sup>1,2</sup>, Susanne Keiding, DMSc<sup>1,2</sup>, Frank V. Mortensen, DMSc<sup>3</sup>, Aage K. O. Alstrup, PhD<sup>1</sup>, Søren B. Hansen, PhD<sup>1</sup>, and Ole L. Munk, Ph

<sup>1</sup>Department of Nuclear Medicine and PET Centre, Aarhus University Hospital, Aarhus, Denmark

<sup>2</sup>Department of Medicine V, Aarhus University Hospital, Aarhus, Denmark

<sup>3</sup>Department of Surgery L, Aarhus University Hospital, Aarhus, Denmark

### Abstract

**Objective**—To determine whether dynamic contrast-enhanced computed tomography (DCE-CT) and the slope method can provide absolute measures of hepatic blood perfusion from hepatic artery (HA) and portal vein (PV) at experimentally varied blood flow rates.

**Materials and Methods**—Ten anesthetized 40-kg pigs underwent DCE-CT during periods of normocapnia (normal flow), hypocapnia (decreased flow), and hypercapnia (increased flow), which was induced by adjusting the ventilation. Reference blood flows in HA and PV were measured continuously by surgically-placed ultrasound transit-time flowmeters. For each capnic condition, the DCE-CT estimated absolute hepatic blood perfusion from HA and PV were calculated using the slope method and compared with flowmeter based absolute measurements of hepatic perfusions and relative errors were analyzed.

**Results**—The relative errors (mean±SEM) of the DCE-CT based perfusion estimates were  $-21\pm 23\%$  for HA and  $81\pm 31\%$  for PV (normocapnia),  $9\pm 23\%$  for HA and  $92\pm 42\%$  for PV (hypocapnia), and  $64\pm 28\%$  for HA and  $-2\pm 20\%$  for PV (hypercapnia). The mean relative errors for HA were not significantly different from zero during hypo- and normocapnia, and the DCE-CT slope method could detect relative changes in HA perfusion between scans. Infusion of contrast agent led to significantly increased hepatic blood perfusion, which biased the PV perfusion estimates.

**Conclusions**—Using the DCE-CT slope method, HA perfusion estimates were accurate at low and normal flow rates whereas PV perfusion estimates were inaccurate and imprecise. At high flow rate, both HA perfusion estimates were significantly biased.

### Keywords

liver perfusion; dynamic CT; slope method; hepatic artery; portal vein

---

In clinical radiology, computed tomography (CT) provides high anatomic resolution and the number of CT examinations continues to increase, but as a tool for functional imaging, CT is still regarded inferior compared with magnetic resonance imaging (MRI) and positron emission tomography (PET).<sup>1</sup> However, recent technical innovations in CT, such as multi-detector row CT systems and new image-reconstruction techniques, have stimulated the use

of tissue blood perfusion estimates based on dynamic contrast-enhanced computed tomography (DCE-CT),<sup>1-3</sup> and DCE-CT is an attractive modality because it is widely available and the examinations are performed much faster than by MRI or PET.

In clinical practice, DCE-CT is mainly used for brain studies,<sup>2</sup> but it has also proven useful for studies of other organs, e.g. for the evaluation of malignant liver tumors,<sup>4</sup> which are predominantly supplied by arterial blood whereas normal liver parenchyma is predominantly supplied by portal venous blood.<sup>5-7</sup> Different methods have been developed to estimate liver perfusion using DCE-CT,<sup>7-17</sup> and the slope methods<sup>10-11</sup> are widely used in clinical practice because they are readily available on workstations provided by the commercial vendors and requires only a relatively short DCE-CT examination, which minimizes the radiation dose to the patient.<sup>2</sup> However, compared to other organs with only arterial blood supply, the liver's dual blood supply from the hepatic artery (HA) and portal vein (PV) complicates the analysis of hepatic DCE-CT data. Following an intravenous bolus injection of a contrast agent, the liver receives first a bolus of the contrast agent through the HA and then a partly overlapping and more dispersed bolus through the PV. Two versions of the slope method are used to estimate liver perfusion. The direct slope method<sup>10</sup> is based on mass conservation (Fick's principle) assuming that there is no outflow of contrast agent into the liver veins during the CT measurement and that the liver DCE-CT data can be divided into two non-overlapping phases from which the individual HA and PV perfusions can be estimated. The subtraction slope method<sup>11</sup> attempts to improve the PV perfusion estimate and is based on the additional assumption that contrast agent in the arteries arrives at the same time in spleen and liver and has similar transit times through liver and spleen. Thus, the spleen DCE-CT data are taken to represent the arterial component of the liver DCE-CT measurements and thus subtracted from the liver DCE-CT data to yield the PV component of the liver DCE-CT data.

DCE-CT data analyzed by the slope method are clinically used for evaluation of the relative differences in the liver perfusion between regions within the same slice, e.g. between malignant liver tumors and surrounding tissue.<sup>4</sup> However, the slope method is based on assumptions that could be violated depending on the flow levels in HA and PV, and it remains to be determined whether DCE-CT and the slope method provide quantitative absolute estimates of hepatic blood perfusion that are needed for cross-sectional (between patients) and longitudinal (follow-up) studies. Thus, the purpose of the present study was to establish whether DCE-CT and the slope method provides absolute measures of the hepatic blood perfusion from the HA and the PV at varying flow levels. This quantitative validation required simultaneous independent measurements of the hepatic blood perfusion, which to our knowledge has not been done before.

## MATERIAL AND METHODS

### Study Design

In ten anaesthetized pigs, we compared DCE-CT estimated HA- and PV-liver tissue blood perfusions at three different flow levels with simultaneous measurements of the hepatic blood perfusions from the HA and PV using highly accurate ultrasound transit-time flowmeters. Changes in the HA- and PV-blood flow rates were experimentally induced by adjusting the ventilation so that three successive periods of normocapnia (normoventilation), hypocapnia (hyperventilation) and hypercapnia (hypoventilation) were obtained (Table 1). The adjusted ventilation was continued until arterial pCO<sub>2</sub> and flowmeter measured blood flow rates in HA and PV became stable. At the end of each capnic condition, a 60 seconds DCE-CT study was performed (Figure 1). Regulated ventilation is a well-established method for reducing cerebral blood flow in patients with severe brain lesions,<sup>18-19</sup> and has been

used in pigs to induce changes in blood flow in the brain<sup>20</sup> and in the splanchnic and portal blood vessels.<sup>21</sup>

### Animal Preparation

Female, 3-month old pigs weighing 38–42 kg (cross-breeds of Danish Landrace and Yorkshire) were fasted for 16 hours with free access to water. The animals were anaesthetized and ventilated as previously described<sup>22</sup> and placed on a thermostatically controlled heating blanket, keeping the rectal temperature between 38.5 and 39.5°C. Catheters (Cordis Corporation, Miami, FL, USA) were inserted into the femoral vein and artery for intravenous infusions and blood sampling, respectively.

The abdomen was opened and ultrasound transit-time flowmeter (MediStim, Oslo, Norway) were placed around the HA and PV. In some cases a bifurcation of the HA was seen and flowmeters were placed around each branch. Arterial blood gasses and acid-base status were measured (ABL, Radiometer, Copenhagen, Denmark) at least every 30 min and adjusted by manipulation of the ventilation (Table 1). After completion of the experiment, the animal was euthanized with an intravenous injection of pentobarbital and the liver was removed. Liver weight and tissue density were measured.

The studies were performed according to the Danish Animal Experimentation Act and the European convention for the protection of vertebrate animals used for experimental and other scientific purposes (ETS No. 123).

### Ultrasound Transit-Time Flowmeter Measurements

Throughout the experiment, blood flow rates (ml blood/min) in the HA and PV were continuously measured by the ultrasound transit-time flowmeters. Infusion of contrast agent was followed by significant alterations in HA- and PV-blood flows. Thus, we choose to use the average blood flow rates in the HA and PV within a 60 second period immediately prior to infusion of the contrast agent as our reference. Furthermore, the average blood flow rates within a 60 second period succeeding DCE-CT acquisition was used to assess the impact of contrast infusion on hepatic perfusion. The values were converted to average liver tissue blood perfusion from each vessel (ml blood/min/ml liver tissue) by correction for liver weight (g) and average liver tissue density (1.05 g/cm<sup>3</sup>) (Winterdahl, unpublished data 2011). The flowmeter measured blood perfusions of the liver tissue from the HA and PV, called “flowmeter measured HA perfusion” and “flowmeter measured PV perfusion”, were used as references for the corresponding DCE-CT estimated values.

### DCE-CT Acquisition

CT acquisition of the first five pigs was performed using a Siemens 16 PET/CT biograph (Siemens AG, Erlangen, Germany) with an axial coverage of 24 mm using collimation 8 × 3 mm; CT acquisition of the last five pigs was performed using a Siemens TruePoint 40 PET/CT biograph (Siemens AG, Erlangen, Germany) with an axial coverage of 28.8 mm using collimation 12 × 2.4 mm.

For each animal, an initial CT acquisition of the entire abdomen was performed following intravenous infusion of 30 ml contrast agent (Visipaque, 270 mg of iodine per ml, temperature 37°C, GE Healthcare A/S, Copenhagen, Denmark) by a power injector (Medrad Inc., Indianola, Pa., USA) at a rate of 4 ml/s. This static scan was performed 1 hour prior to the first dynamic CT acquisition and was used to identify the location of the PV. The CT field-of-view was centered at the position of PV and kept in this position throughout the study. Dynamic CT measurements were acquired for 60 seconds. Contrast agent was administered by power injector as an intravenous infusion of 30 ml in the course of 6

seconds. In the first five animals, the dynamic CT acquisition was started simultaneously with the start of the contrast agent infusion, and in the last five animals it was started five seconds before. Imaging parameters were 360°/s tube rotation, 120 kV tube voltage, 200 mA tube current, 512×512 matrix, axial slice thickness 3 mm, field of view 500 mm, and sampling interval one image/s. Longer sampling intervals (>1 image/s) are known to bias perfusion estimates using the slope method.<sup>23</sup> Images were reconstructed using a smooth conventional kernel, B30s (Siemens AG, Erlangen, Germany).

### Image Analysis

In each animal, volumes of interest (VOIs) were drawn in the central parts of the aorta (median, 0.77 cm<sup>3</sup>; range, 0.72–0.83 cm<sup>3</sup>), PV (1.48 cm<sup>3</sup>; 1.21–1.76 cm<sup>3</sup>) and in the liver tissue (30 cm<sup>3</sup>; 18–46 cm<sup>3</sup>) (Figure 2). In four animals, a spleen VOI could be drawn (1.55 cm<sup>3</sup>; 1.39–1.76 cm<sup>3</sup>). Aorta, PV and spleen VOIs were drawn in two axial slices where as the liver VOI was drawn in three or four slices, depending on size and vasculature of the liver. VOIs were drawn using the DynEva software tool (Siemens, Forchheim, Germany). We carefully accounted for three things in the drawing procedure. Firstly, to make the VOIs as large as possible to minimize noise but with a sufficient margin from the edge of the structures to minimize partial-volume effects due to respiratory motion. Secondly, to exclude areas with beam hardening due to effects of the bolus injection or close proximity to the flowmeters (in a few cases, 1 out of 60 images was removed from the dynamic series). Thirdly, to avoid inclusion of larger intra-hepatic blood vessels close to the porta hepatis. For each DCE-CT acquisition, we repeated the entire process of drawing the VOIs four times to address the reproducibility of the procedure. Each dynamic series was manually inspected right after acquisition as well as in the VOI drawing process, with special attention to the localization of the PV. For each animal, the same set of VOIs was used for all three CT acquisitions. The CT numbers (HU) were subtracted by the average pre-contrast CT number (HU) to obtain the relative enhancement ( $\Delta$ HU) and a time course of the relative enhancement ( $\Delta$ HU(t)) was generated for each VOI.  $\Delta$ HU is proportional to the concentration of contrast agent with a proportionality constant that is the same for blood and liver tissue.<sup>24</sup> We avoided decreased peak enhancement and broadening of the aorta- $\Delta$ HU(t) (Figure 3 A) and PV- $\Delta$ HU(t) (Figure 3 B) due to excessive spatial averaging by defining the aorta VOI using only one or two axial slices. Remaining analysis was implemented in custom made IDL software (Research Systems Inc., Boulder, CO, USA) Gamma-variate functions<sup>25</sup> were fitted to  $\Delta$ HU(t) from the aorta, PV and spleen to reduce noise and allow a better estimate of the maximum relative enhancement used.

### DCE-CT Estimated HA Perfusion

The DCE-CT estimated HA perfusion was calculated as the maximum slope of the HA phase of the bi-phasic liver- $\Delta$ HU(t) (Figure 3 C) divided by the peak of the aorta- $\Delta$ HU(t).<sup>10</sup> The maximum slope of this initial part of the liver- $\Delta$ HU(t) was estimated by a linear fit to at least three data points and with a goodness of fit assessed by the coefficient of determination  $R^2 > 0.90$ , thereby avoiding the inclusion of excessive data points that could have led to underestimation of the slope. This DCE-CT estimated blood perfusion of the liver tissue from the HA using the slope method was denoted “DCE-CT estimated HA perfusion”.

### DCE-CT Estimated PV Perfusion

The PV perfusion was calculated by two versions of the slope method: the direct slope method and the subtraction slope method. The maximum slopes were determined using the same criteria as for HA, and the DCE-CT estimated blood perfusions of the liver tissue from the PV using the direct slope method was denoted “DCE-CT estimated PV perfusion”.

- Direct slope method.<sup>10</sup> The time point of the initial rise of the PV- $\Delta$ HU(t) was used to separate the HA- and PV-phases of the liver- $\Delta$ HU(t) whereas Miles<sup>10</sup> and co-worker used peak splenic enhancement to separate the two phases. However, the maximum arterial and portal slopes for the time course of the liver relative enhancement are relatively well separated, as shown in Figure 3 C. The PV perfusion was calculated as the maximum slope of the PV phase of the liver- $\Delta$ HU(t) divided by the value of the peak of the PV- $\Delta$ HU(t).
- Subtraction slope method.<sup>11</sup> In the four animals where a spleen VOI could be defined and the time point of the peak of the spleen- $\Delta$ HU(t) was estimated from a gamma-variate fit and used to separate the HA- and PV-phases of the liver- $\Delta$ HU(t). The ratio of HA liver perfusion to (arterial) spleen perfusion was estimated as the maximum slope of the HA phase of the liver- $\Delta$ HU(t) divided by the maximum slope of the spleen- $\Delta$ HU(t). The arterial component of the liver- $\Delta$ HU(t) was calculated as the gamma-variate fit of the spleen- $\Delta$ HU(t) multiplied by the ratio of the HA perfusion to the spleen perfusion. The corresponding PV component of the liver- $\Delta$ HU(t) was calculated by subtracting the HA component from the liver- $\Delta$ HU(t) and the PV perfusion was then estimated as the maximum slope of the PV component of the liver- $\Delta$ HU(t) divided by the peak of the PV- $\Delta$ HU(t).

### Statistical Analysis

Normally distributed data were reported as the mean  $\pm$  standard error of the mean (SEM) and otherwise as the median and range. The relative error of the DCE-CT estimated hepatic blood perfusion was defined as the difference between the DCE-CT estimated hepatic blood perfusion and the flowmeter measured hepatic blood perfusion divided by the flowmeter measured hepatic blood perfusion. The mean and SEM of the relative errors of the DCE-CT estimated hepatic blood perfusions were interpreted as measures of accuracy and precision of the DCE-CT method, respectively. Analysis of variance (ANOVA) was used in a repeated measures design (three different capnic conditions in each pig), allowing us to account for multiple measurement in one animal. Furthermore, the use of ANOVA allowed us to separate the observed total variance of the relative errors of the DCE-CT estimates into components attributable to different sources of variation. Linear regression was used to describe the dependence of DCE-CT estimates on the measured flowmeter perfusions. Slopes and Y-intercepts are given with 95% confidence intervals (CI). Spearman's rank correlation coefficient was used as a measure of statistical dependence between DCE-CT estimated hepatic absolute blood perfusion and the flowmeter measured absolute hepatic blood perfusion. Statistical significance was set at  $P < 0.05$ .

## RESULTS

### Capnic Conditions

The flowmeter measured absolute HA- and PV-blood flow rates during the DCE-CT measurements were 0.20 l/min and 0.55 l/min (median values), respectively, at normocapnia (Table 1). During hyperventilation, hypocapnia developed and the HA- and PV-blood flow rates both decreased gradually and reached a steady level around 75% and 93%, respectively, of the normocapnia values (Figure 1 and Table 1). During hypoventilation, hypercapnia developed and the HA- and PV-blood flow rates both increased during the first hour. Hereafter, the PV blood flow continued to increase to a steady level whereas the HA blood flow was steady or decreased slightly. We let hypercapnia develop as much as possible in order to have an experimental range of the measurements as wide as possible while keeping physiological control parameters reasonably constant. At the end of the hypercapnic condition, the HA- and PV-blood flow rates were around 105% and 163%, respectively, of the normocapnia values (Figure 1 and Table 1).

## Impact of Contrast Infusion on Hepatic Perfusion

Estimates of HA perfusions required data from the first 30 seconds, whereas the estimation of the PV perfusions required the full 60 seconds acquisition period. As shown in Figure 4 A, infusion of the contrast agent was followed by significant increments of measured HA- and PV-blood flows in each of the 30 measurements. HA blood flow increased 23 seconds (18–25 seconds) after start of the 6 second contrast agent infusion, and PV blood flow increased after 35 seconds (31–37 seconds). HA- and PV-flows remained at peak levels for a few seconds and then decreased to steady levels that, compared to the pre-contrast level, were increased by 12% (–2–25%) for the HA and 18% (–7–46%) for the PV ( $P < 0.001$  for both HA and PV) (Figure 4B). Thus, the hepatic blood perfusion was significantly changed by the DCE-CT procedure itself. The DCE-CT estimated HA perfusion was calculated using DCE-CT data up to around 30 seconds after start of the infusion of the contrast agent and was accordingly almost not influenced by the contrast agent induced flow changes. However, the DCE-CT estimated PV perfusion was based on DCE-CT data up to around 55 seconds after start of the contrast agent infusion and was accordingly biased significantly due to the artificially increased PV flow.

### DCE-CT acquisition

Different axial coverage has been reported to influence perfusion estimates.<sup>26</sup> However, the two CT imaging systems applied in this study had very similar axial coverage (24 mm and 28.8 mm respectively). In the last five animals the scan was started five seconds before contrast infusion. However, there was no statistically significant differences between the relative errors of HA and PV estimates obtained in the first five animals and the last five animals (t-test;  $P = 0.25$  and  $P = 0.49$  respectively). Thus, data from the two scanners were pooled to increase statistical power.

### DCE-CT Estimated HA Perfusion

During normocapnia, hypocapnia and hypercapnia conditions absolute estimates of HA perfusion using the slope method were 0.19 (0.04–0.53) l blood/min, 0.15 (0.07–0.310) l blood/min and 0.21 (0.04–0.70) l blood/min respectively. The DCE-CT estimated HA perfusion was positively correlated to the flowmeter measured HA perfusion but with large variations (Figure 5A). The linear regression had a slope of 1.08 (95% CI: 0.58 to 1.58) that was not significantly different from unity, and a Y-intercept of 0.022 (95% CI: –0.11 to 0.16) that was not significantly different from zero. Spearman's rank correlation coefficient was 0.622 ( $P = 0.0002$ ). During normocapnia and hypocapnia, the DCE-CT estimated HA perfusions were accurate and the mean relative error was not significantly different from zero, but during hypercapnia the DCE-CT estimated HA perfusions were overestimated with a mean relative error significantly larger than zero (Table 2). The precision of the DCE-CT estimated HA perfusion was not significantly different between the capnic conditions.

### DCE-CT Estimated PV Perfusion – Direct Slope Method

For the DCE-CT estimation of the PV perfusion, the direct method could be used in all pigs and capnic conditions ( $n = 30$ ). During normocapnia, hypocapnia and hypercapnia conditions absolute estimates of PV perfusion using the direct method were 0.541 (0.399–1.200) l blood/min, 0.504 (0.280–0.910) l blood/min and 0.900 (0.360–1.840) l blood/min respectively. The DCE-CT estimated PV perfusion did not correlate with the flowmeter measured PV perfusion. The linear regression had a slope of 0.011 (95% CI: –0.44 to 0.46) that was not significantly different from zero, a Y-intercept of 0.91 (95% CI: 0.55 to 1.28). Spearman's rank correlation coefficient was –0.0628 ( $P = 0.7$ ). During hypercapnia, the DCE-CT estimated PV perfusion was accurate and the mean relative error was not significantly different from zero, but during normocapnia and hypocapnia the estimates were

overestimated with a mean relative error significantly larger than zero (Table 2). The precision of the DCE-CT estimated PV perfusion was not significantly different between the capnic conditions.

### Reproducibility of DCE-CT Estimated HA and PV Perfusion

To assess reproducibility, the total variation associated with relative errors of the DCE-CT estimates of the HA and PV perfusions were divided into three components. 60% of the total variation associated with the DCE-CT estimated HA perfusion was due to variation between animals and 18% was due to variation within animals (i.e. between capnic conditions). 45% of the total variation associated with the DCE-CT estimated PV perfusion was due to variation between animals and 16% was due to variation within animals. The entire process of drawing e.g. the liver VOIs contains an element of subjectivity. The VOIs have to be large but at the same time avoiding e.g. inclusion of larger intra-hepatic blood vessels. However, the use of different liver tissue VOIs only accounted for 0.2% and 1.2% of total variation of the DCE-CT estimated HA and PV perfusion, respectively. The three components accounted for 79% of the total variation for HA and only 62% for PV, indicating that the slope method is better for estimating HA perfusion than for PV perfusion. Figure 5B illustrates the relationship between the absolute changes in the DCE-CT estimated HA perfusion and the flowmeter measured HA perfusion between capnic conditions. Linear regression showed a slope of 1.65 (95% CI: 1.23 to 2.06), a Y-intercept of 0.12 (95% CI: 0.059 to 0.175). Spearman's rank correlation coefficient was 0.837 ( $P < 0.00001$ ). The reproducibility within animals was 9.4% and 14.3% for the relative error of DCE-CT estimates of HA and PV, respectively, when excluding between animal variations.

### DCE-CT Estimated PV Perfusion – Subtraction Slope Method

In the four animals where the PV perfusion could be estimated using both the direct slope method and the subtraction slope method (Table 3), the subtraction slope method gave significantly higher estimates of the PV perfusion than the direct slope method ( $P = 0.004$ ) and the mean relative error was significantly higher ( $P < 0.001$ ). Thus, based on these four animals, the subtraction method was more inaccurate than the direct method, but the precisions of the two slope method versions were equally poor.

## DISCUSSION

The DCE-CT slope method is widely used to quantify blood perfusion in the brain and other organs with a single arterial blood supply. For the liver, however, the two supplying vessels complicate the analysis of hepatic perfusion. First, the liver receives a bolus of contrast agent through the HA and later a more dispersed bolus through the PV. If the supply from the two vessels had been truly bi-phasic, the liver would be completely empty of HA-supplied contrast agent before the PV-supply arrives, and then the direct slope method should in principle work equally well for the liver as for the brain. However, in practice the supply of contrast agent from the HA and PV overlap in the liver and accordingly the signal from the liver is not bi-phasic.

We used an experimental setup with continuous flowmeter measurements of the hepatic blood perfusion that allowed us to validate the perfusion estimates using the DCE-CT slope method at varying flow levels. The slope method based perfusion estimates were compared to independent measurements acquired immediately before DCE-CT acquisition using transit-time flowmeters. We quantified the accuracy and precision of the perfusion estimates and found that they were flow-dependent. The DCE-CT estimated HA perfusion was accurate during normocapnia and hypocapnia (low and normal flow) and could correctly detect absolute changes in the HA perfusion between two capnic conditions within the same

animal. Whereas the DCE-CT estimated PV perfusion were inaccurate and imprecise. Thus, we found that between-scan comparisons of the hepatic perfusion estimated by the DCE-CT slope method were of limited use, except for studies of the HA perfusion. Nevertheless, our findings do not contradict that the DCE-CT slope method can be useful to evaluate relative differences in the liver perfusion between regions within the same scan, which is the most commonly used clinical application.

### Experimental Model

We used 40-kg pigs because they have a body size allowing use of a human CT-scanner, their liver and vessel sizes are comparable to those of humans, and their hepatic vasculature is similar to that of humans.<sup>27–28</sup> The animals are sufficiently robust to allow for anesthesia and surgery and use of several experimentally induced distinct flow levels within the same animal. The only drawback is their tongue-shaped spleen, which we could only identify within the field-of-view in four out of ten animals. In humans, the spleen is often included in field-of-view, which may make the subtraction slope method for the estimation of the PV perfusion more applicable in humans than in pigs. However, based on the four animals where the spleen could be identified, we found that the direct slope method was more accurate than the subtraction slope method for estimation of the PV perfusion.

We used the ultrasound transit-time flowmeter as reference method because it measures volume of blood flow with high accuracy around 1%<sup>29</sup> and with high precision (see Figure 4A). In separate experiments, we validated the linearity of the flowmeters up to 2 l/min, and validated that they measured equally accurate with and without contrast agent in the blood (Winterdahl, unpublished data 2012). As the present flowmeter measured HA- and PV-perfusions were obtained by dividing the measured HA- and PV-blood flow rates by the weight of the liver, the flowmeter method yielded measurements of the global liver perfusion, whereas the DCE-CT method yielded estimates of the regional liver blood perfusion. Since our DCE-CT estimated perfusions were calculated on the basis of CT liver VOIs drawn as large as possible, it is reasonable to assume that the DCE-CT estimated perfusion reflected the global liver perfusion.

In two previous pig studies, we validated estimates of the total hepatic blood perfusion (HA +PV) at normocapnia using dynamic PET.<sup>30,31</sup> In these studies, we also used pigs weighing 40 kg and similar surgical procedures and compared PET estimated regional liver blood perfusion in a large VOI with ultrasound transit-time flowmeter measured perfusion. The relative error of the PET estimated total liver blood perfusion in these studies,  $8\pm 9\%$ ,<sup>30,31</sup> was significantly more accurate and precise than the value of  $57\pm 26\%$  obtained by the present DCE-CT method (Table 2). Differences in the precision between the two modalities may partly be explained by differences in VOI size. However, this cannot explain differences in the accuracy. Thus, we are confident that the large relative errors of the DCE-CT estimated HA- and PV-perfusions were caused by the slope method and neither by the experimental setup nor by the use of ultrasound transit-time flowmeters as the reference method.

### Assumptions of the Slope Method

The slope method assumes that there is no wash-out of contrast agent in the liver vein before the liver- $\Delta HU(t)$  reaches its maximum slope. This assumption was violated at high perfusion rates in the present study, in agreement with another study,<sup>32</sup> leading to underestimation of the maximum slope and consequently to an underestimation of the liver tissue blood perfusion.<sup>9</sup> However, we found that this effect only contributed in minor degree to the uncertainty of the DCE-CT estimated perfusion because the mean relative errors of the DCE-CT estimated perfusion were not significantly underestimated in any cases (Table



2). The DCE-CT method overestimated the PV perfusion at normocapnia and hypocapnia (Tables 2 and 3). Thus, the violation of the no venous outflow assumption, which should be most pronounced at high perfusion rates at hypercapnia (Table 1), actually led to more accurate PV perfusion estimates at hypercapnia for both the direct and the subtraction method (Tables 2 and 3). The slope method further assumes that the bi-phasic liver- $\Delta$ HU(t) can be divided into a HA phase followed by PV phase. We found that this assumption could be violated even at normal perfusion rates. Whereas the subtraction method<sup>11</sup> attempts to remove the HA component of the liver- $\Delta$ HU(t) to derive a corrected PV phase liver- $\Delta$ HU(t), no method removes an unwanted PV component of the liver- $\Delta$ HU(t) to derive a corrected HA phase liver- $\Delta$ HU(t). The contribution of contrast agent through the PV during the HA phase effectively increased the slope of the liver- $\Delta$ HU(t) and in turn led to an overestimated HA perfusion. This effect was most pronounced during hypercapnia, at high PV perfusion, where the transit time, defined as blood volume divided by blood flow, through the PV is short (Table 2). These limitations of the slope method are probably equally problematic for human studies because the mean transit time of blood from aorta to PV and the mean hepatic transit time are similar in pigs and humans.<sup>33</sup> Recent development of biological phantoms for DCE-CT may allow some of the aforementioned limitations to be addressed systematically.<sup>34, 35</sup>

### Effect of Respiratory Motion

The PV- $\Delta$ HU(t) is particularly prone to partial volume effects because the PV is orientated mostly perpendicular to the respiratory motion. The artifact can be reduced by shorter CT rotation times and restricted breathing. During normocapnia, the pigs were ventilated using a relatively large tidal volume (Table 1) mimicking normally breathing patients. Thus, partial volume caused an underestimation of the PV- $\Delta$ HU(t) peak, which led to an overestimated PV perfusion (Table 2). In contrast, the accuracy of PV perfusion was significantly better during hypercapnia where the pigs were ventilated using a small tidal volume. However, this improved accuracy at hypercapnia was probably a combined effect of shallow breathing and the violation of the assumption of no venous outflow. Thus, the results indicate a potential benefit of instructing the patients to breathe shallow during the 60 second DCE-CT acquisition.

### Contrast Agent Administration Increases the Hepatic Blood Flow

The observed increase in HA- and PV-perfusion around 30 seconds after injection of the contrast agent (Figure 4A) may be ascribed to a systemic vasodilating effect of the contrast agent on arteries as shown for the coronary arteries,<sup>37</sup> but the underlying mechanism remains unresolved.<sup>38</sup> As far as we know, it has not been shown previously that administration of contrast agent in itself led to significantly increased hepatic blood perfusion from both vessels. Actually, such effects have been believed not to be substantial within the first pass of intravenously administered contrast agents, especially working with low-osmolality contrast agents.<sup>9</sup> It is a fundamental problem for the slope method that the determination of the maximum slope of the liver- $\Delta$ HU(t) includes data points after the contrast agent-induced increase in flow, which imposes an unavoidable inherent bias on the DCE-CT methods when estimating PV perfusion. The prolonged nature of the elevated HA- and PV-blood flow rates induced by the contrast agent is in accordance with its long half-life in the body. Thus, it is not possible to perform two DCE-CT examinations within a short interval without the first one interfering with the second.

## CONCLUSIONS

We found that the DCE-CT slope method could estimate the absolute HA perfusion accurately at normal perfusion rates and that absolute changes in the HA liver tissue

perfusion could be detected. However, the estimates of hepatic blood perfusion using the DCE-CT slope method were biased by inherent limitations. The slope method assumes that there is no outflow of contrast agent into the liver veins before the liver- $\Delta$ HU(t) reaches a maximum slope and that a bi-phasic liver- $\Delta$ HU(t) can be separated into HA- and PV-phases. When these assumptions were violated at high perfusion rates, the accuracy and precision of the absolute DCE-CT estimated hepatic perfusion estimates were poor.

## Acknowledgments

This study was supported by the National Institute of Diabetes and Digestive and Kidney Diseases (R01-DK074419), the Danish Medical Research Council (09-061564;09-073658), the Novo Nordic Foundation (R121-A10313), Aase and Ejnar Danielsen's Foundation (106309), Helga and Peter Korning's Foundation, and the A. P. Møller Foundation for the Advancement of Medical Science. We thank D.F. Smith for language revision.

## REFERENCES

1. Fink C, Brix G, Halliburton SS, et al. Functional computed tomography. *Invest Radiol.* 2012; 47:1. [PubMed: 22178892]
2. Brix G, Lechel U, Petersheim M, et al. Dynamic contrast-enhanced CT studies: balancing patient exposure and image noise. *Invest Radiol.* 2011; 46:64–70. [PubMed: 20881865]
3. Grüner JM, Paamand R, Højgaard L, et al. Brain perfusion CT compared with  $^{15}\text{O}$ - $\text{H}_2\text{O}$ -PET in healthy subjects. *EJNMMI Res.* 2011; 1:28. [PubMed: 22214473]
4. Goetti R, Reiner CS, Knuth A, et al. Quantitative perfusion analysis of malignant liver tumors: dynamic computed tomography and contrast-enhanced ultrasound. *Invest Radiol.* 2012; 47:18–24. [PubMed: 21788906]
5. Itai Y, Matsui O. Blood flow and liver imaging. *Radiology.* 1997; 202:306–314. [PubMed: 9015047]
6. Wiering B, Ruers TJ, Krabbe PF, et al. Comparison of multiphase CT, FDG-PET and intra-operative ultrasound in patients with colorectal liver metastases selected for surgery. *Ann Surg Oncol.* 2007; 14:818–826. [PubMed: 17136470]
7. Pandharipande PV, Krinsky GA, Rusinek H, et al. Perfusion imaging of the liver: current challenges and future goals. *Radiology.* 2005; 234:661–673. [PubMed: 15734925]
8. Miles KA. Perfusion CT for the assessment of tumour vascularity: which protocol? *Br J Radiol.* 2003; 76:S36–S42. [PubMed: 15456712]
9. Miles KA, Griffiths MR. 2003 Perfusion CT: a worthwhile enhancement? *Br J Radiol.* 2003; 76:220–231. [PubMed: 12711641]
10. Miles KA, Hayball MP, Dixon AK. Functional images of hepatic perfusion obtained with dynamic CT. *Radiology.* 1993; 188:405–411. [PubMed: 8327686]
11. Blomley MJ, Coulden R, Dawson P, et al. Liver perfusion studied with ultrafast CT. *J Comput Assist Tomogr.* 1995; 19:424–433. [PubMed: 7790553]
12. Materne R, Van Beers BE, Smith AM, et al. Non-invasive quantification of liver perfusion with dynamic computed tomography and a dual-input one-compartmental model. *Clin Sci.* 2000; 99:517–525. [PubMed: 11099395]
13. Kapanen MK, Halavaara JT, Häkkinen AM. Open four-compartment model in the measurement of liver perfusion. *Acad Radiol.* 2005; 12:1542–1550. [PubMed: 16321743]
14. Cao Y, Platt JF, Francis IR, et al. The prediction of radiation-induced liver dysfunction using a local dose and regional venous perfusion model. *Med Phys.* 2007; 34:604–612. [PubMed: 17388178]
15. Cuenod C, Leconte I, Siauve N, et al. Early changes in liver perfusion caused by occult metastases in rats: detection with quantitative CT. *Radiology.* 2001; 218:556–561. [PubMed: 11161178]
16. Stewart EE, Chen X, Hadway J, et al. Correlation between hepatic tumor blood flow and glucose utilization in a rabbit liver tumor model. *Radiology.* 2006; 239:740–750. [PubMed: 16621929]
17. Stewart EE, Chen X, Hadway J, et al. Hepatic perfusion in a tumor model using DCE-CT: an accuracy and precision study. *Phys Med Biol.* 2008; 53:4249–4267. [PubMed: 18653923]

18. Marrubini G, Bozza ML. Chemico-toxicological diagnosis in complications of anesthesia. *Minerva Medicoleg.* 1961; 81:166–167. [PubMed: 13767138]
19. Gordon E, Rossanda M. The importance of the cerebrospinal fluid acid-base status in the treatment of unconscious patients with brain lesions. *Acta Anaesthesiol Scand.* 1968; 12:51–73. [PubMed: 5709578]
20. Olsen AK, Keiding S, Munk OL. Effect of hypercapnia on cerebral blood flow and blood volume in pigs studied by positron emission tomography. *Comp Med.* 2006; 56:416–420. [PubMed: 17069026]
21. Karlsson T, Stjernstrom EL, Stjernstrom H, et al. Central and regional blood flow during hyperventilation. An experimental study in the pig. *Acta Anaesthesiol Scand.* 1994; 38:180–186. [PubMed: 8171955]
22. Winterdahl M, Keiding S, Sørensen M, et al. Tracer input for kinetic modelling of liver physiology determined without sampling portal venous blood in pigs. *Eur J Nucl Med Mol Imaging.* 2011; 38:263–270. [PubMed: 20882283]
23. Kloska SP, Fischer T, Sauerland C, et al. Increasing sampling interval in cerebral perfusion CT: Limitations for the maximum slope method. *Acad Radiol.* 2010; 17:61–66. [PubMed: 19734063]
24. Brix G, Bahner ML, Hoffmann U, et al. Regional blood flow, capillary permeability, and compartmental volumes: measurement with dynamic CT - initial experience. *Radiology.* 1999; 210:269–276. [PubMed: 9885619]
25. Starmer CF, Clark DO. Computer computations of cardiac output using the gamma function. *J Appl Physiol.* 1970; 28:219–220. [PubMed: 4905082]
26. Ng QS, Goh V, Klotz E, et al. Quantitative assessment of lung cancer perfusion using MDCT: does measurement reproducibility improve with greater tumor volume coverage? *Am J Roentgenol.* 2006; 187(4):1079–1084. [PubMed: 16985160]
27. Court FG, Wemyss-Holden SA, Morrison CP, et al. Segmental nature of the porcine liver and its potential as a model for experimental partial hepatectomy. *Br J Surg.* 2003; 90:440–444. [PubMed: 12673745]
28. Farinon AM, Zannoni M, Lampugnani R, et al. Surgical anatomy of the liver and bile ducts in the most common experimental animals. *Chir Patol Sper.* 1981; 29:215–231. [PubMed: 7052793]
29. Mortensen FV, Rasmussen JS, Viborg O, et al. Validation of a new transit time ultrasound flowmeter for measuring blood flow in colonic mesenteric arteries. *Eur J Surg.* 1998; 164:599–604. [PubMed: 9720937]
30. Munk OL, Bass L, Roelsgaard K, et al. Liver kinetics of glucose analogs measured in pigs by PET: importance of dual-input blood sampling. *J Nucl Med.* 2001; 42:795–801. [PubMed: 11337579]
31. Winterdahl M, Munk OL, Sørensen M, et al. Hepatic blood perfusion measured by 3-minute dynamic 18F-FDG PET in pigs. *J Nucl Med.* 2011 Jul; 52(7):1119–1124. Epub 2011 Jun 16. [PubMed: 21680685]
32. Lee TY, Purdie TG, Stewart E. CT imaging of angiogenesis. *J Nucl Med.* 2003; 47:171–187.
33. Munk OL, Keiding S, Bass L. Impulse-response function of splanchnic circulation with model-independent constraints: theory and experimental validation. *Am J Physiol Gastrointest Liver Physiol.* 2003; 285:G671–G680. [PubMed: 12686507]
34. Thompson SM, Ramirez-Giraldo JC, Knudsen B, et al. Porcine ex vivo liver phantom for dynamic contrast-enhanced computed tomography: development and initial results. *Invest Radiol.* 2011; 46:586–593. [PubMed: 21610506]
35. Haberland U, Cordes J, Lell M, et al. A biological phantom for contrast-media-based perfusion studies with CT. *Invest Radiol.* 2009; 44(10):676–682. [PubMed: 19724231]
36. Crystal GJ, Salem MR. Investigations into the mechanisms of coronary vasodilation by contrast media in dogs. *Invest Radiol.* 1996; 31:556–562. [PubMed: 8877492]
37. Narishige T, Egashira K, Akatsuka Y, et al. Effects of iomeprol, a new nonionic contrast medium, vis a vis iopamidol and nitroglycerin, on coronary diameter and blood flow in chronically instrumented dogs. *Cardiovasc Intervent Radiol.* 1993; 16:343–347. [PubMed: 8131164]

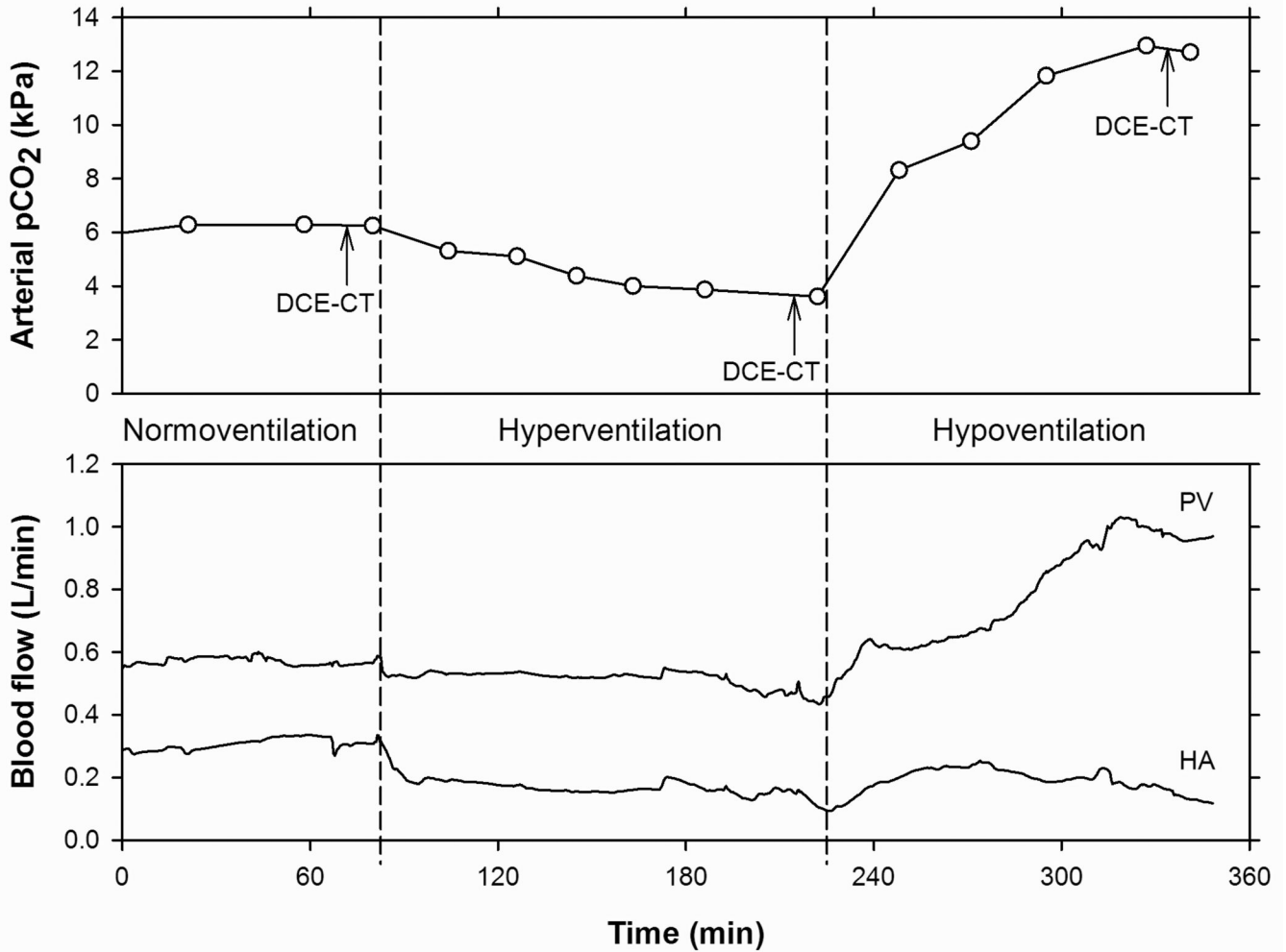


**Figure 1.**

Experimental design: each pig experiment comprised three successive capnic conditions, induced by variations in the ventilation: Normoventilation (normocapnia), hyperventilation (hypocapnia), and hypoventilation (hypercapnia). Top: Time course of arterial blood pCO<sub>2</sub> with measurements (○) connected by straight lines. DCE-CT was acquired in the end of each capnic condition, indicated by arrows. Bottom: Time courses of blood flow rates in portal vein (PV) and hepatic artery (HA) measured by ultrasound transit-time flowmeters. Total duration of the entire experiment was approximately eight hours.

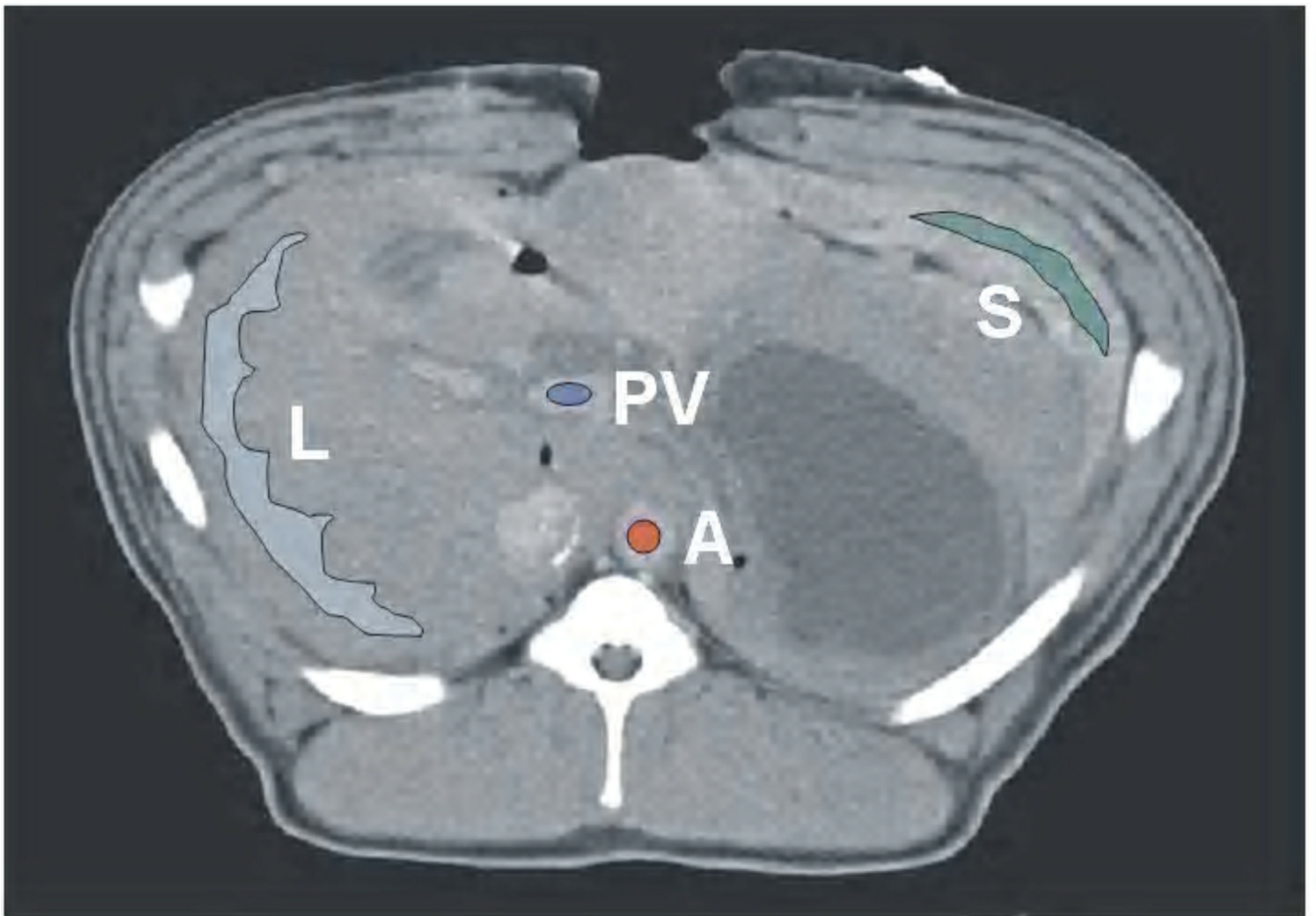


**Figure 2.** Transaxial slice of CT image of the upper abdomen. Volumes of interest (VOIs) were drawn within the aorta (A), portal vein (PV), liver (L), and spleen (S).

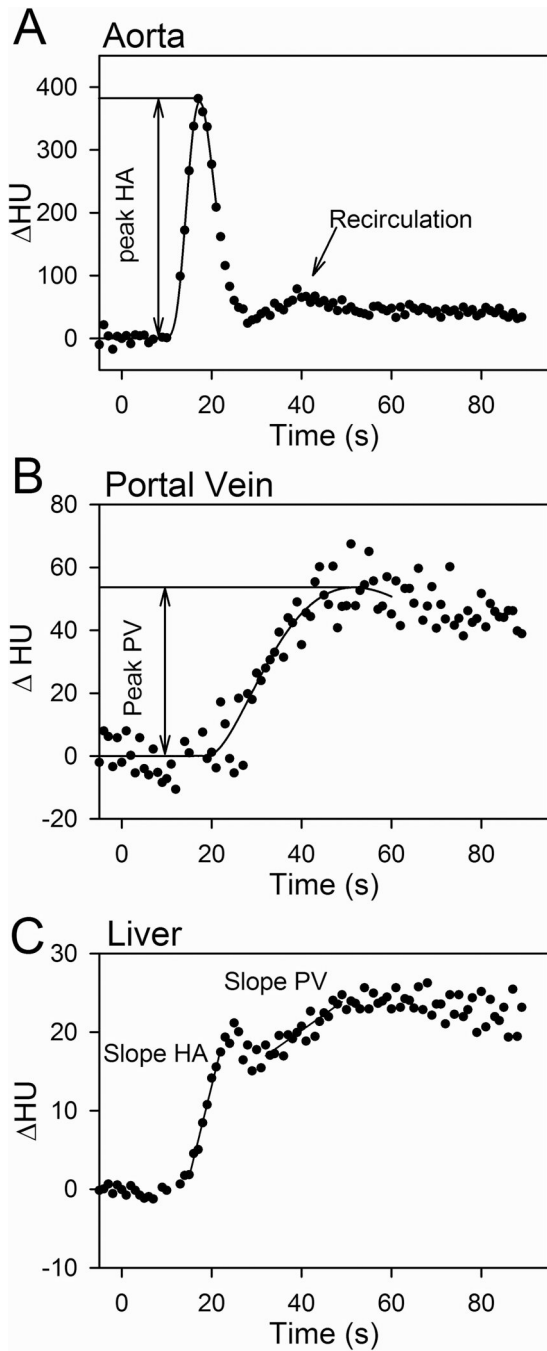


**Figure 3.**

Slope method estimation of absolute HA- and PV-liver blood perfusions by the direct method. Contrast agent was infused at  $t=0$  seconds. Time courses show the relative enhancement,  $\Delta HU(t)$ , in aorta (A), portal vein (B), and liver tissue (C). Curves in (A) and (B) are gamma-variate functions fitted to the measurements (●) and used to estimate the peak  $\Delta HU(t)$  values. The maximum slopes of the arterial (HA slope) and the portal phases (PV slope) were fitted to the liver- $\Delta HU(t)$  in the two phases. The aorta- $\Delta HU(t)$  shows recirculating contrast agent.

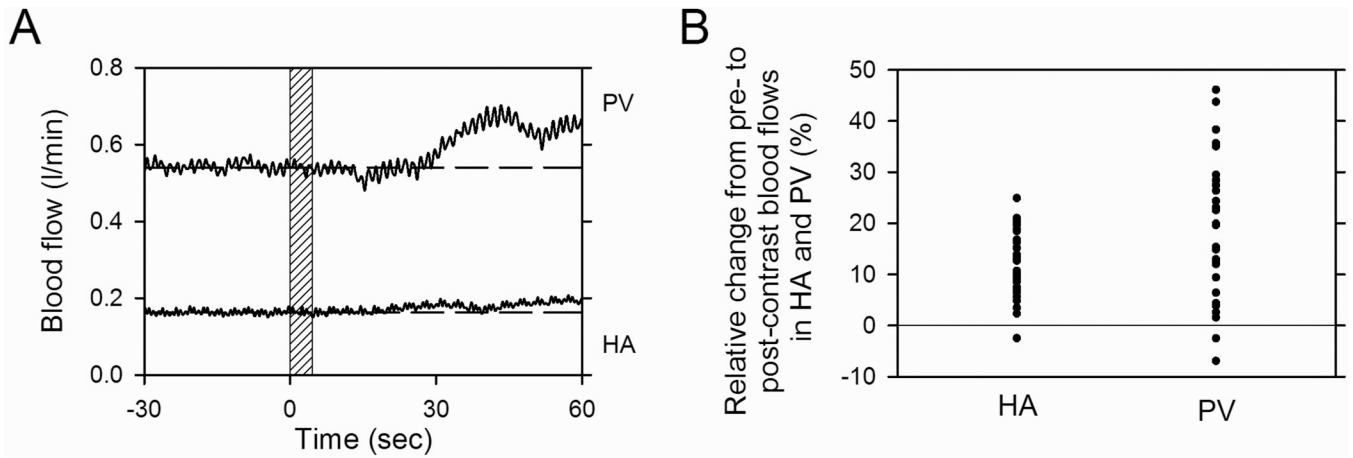


**Figure 4.**

Example of blood flow rates in the portal vein (PV) and hepatic artery (HA) measured continuously by ultrasound transit-time flowmeters before, during and after a 6 second intravenous infusion of CT contrast agent starting at time zero (box) (A). Dashed lines show extrapolated average pre-contrast values. It is seen that the flowmeter measurements are precise and able to detect the pulsatile blood flow rates. Relative change from pre- to post-contrast blood flows in HA and PV for all 30 administrations of contrast agent (B).

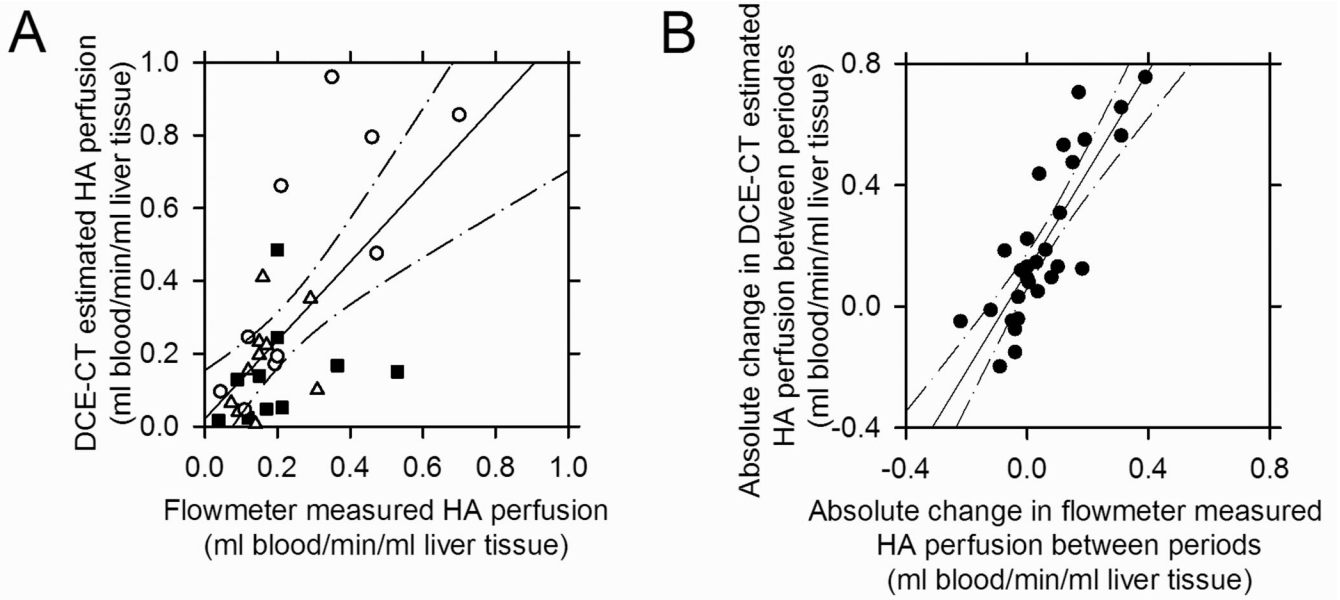


**Figure 5.**

Relationship between DCE-CT estimated HA liver tissue perfusions and flowmeter measured HA liver tissue perfusions in 10 pigs at normocapnia (■), hypocapnia (△) and hypercapnia (○) (totally 30 capnic conditions) (A). Relationship between absolute changes in DCE-CT estimated HA liver tissue perfusion and absolute change in flowmeter measured HA liver tissue perfusions between the capnic conditions (●) (B). Linear regression lines and the 95% confidence intervals are shown.



TABLE 1

Experimental design.

	Capnic Condition		
	Normocapnia	Hypocapnia	Hypercapnia
Adjustable ventilator parameters			
Breaths per minute	15–18	25–40	6–10
Tidal volume [ml]	250–300	275–340	110–175
Ratio of O <sub>2</sub> and atmospheric air	0.3–0.4	0.2–0.4	0.5–1.0
Measured physiological parameters			
Arterial pCO <sub>2</sub> [kPa]	6.5 (5.6–7.6)	3.4 (2.5–4.4)	16.8 (12.1–22.0)
Heart rate [bpm]	82 (60–131)	89 (85–160)	186 (64–213)
Blood pressure	143/103	116/95	168/92
Systolic/diastolic [mmHg]	(125–169/82–152)	(72–152/62–121)	(80–207/43–117)
pH	7.42 (7.32–7.49)	7.51 (7.29–7.60)	7.11 (6.86–7.87)
HA flow [l blood/min]	0.20 (0.03–0.53)	0.15 (0.07–0.29)	0.21 (0.03–0.70)
PV flow [l blood/min]	0.55 (0.40–1.20)	0.51 (0.28–0.91)	0.90 (0.36–1.84)
HA + PV flow [l blood/min]	0.70 (0.44–1.73)	0.69 (0.43–1.16)	1.28 (0.48–2.05)
HA/(HA+PV)	0.3 (0.1–0.4)	0.2 (0.1–0.7)	0.2 (0.1–0.4)

Values are shown as range or median (range) from studies in 10 pigs; pCO<sub>2</sub>, partial carbon dioxide tension in arterial blood; HA, hepatic artery; PV, portal vein.

**TABLE 2**

Relative error of DCE-CT estimated liver tissue blood perfusion using the direct slope method compared with flowmeter measured liver tissue blood perfusions.

	Capnic Condition		
	Normocapnia	Hypocapnia	Hypercapnia
HA	-21 ± 23%	9 ± 23%	64 ± 28% *
PV	81 ± 31% *	92 ± 42% *	-2 ± 20%
HA+PV	57 ± 26%	72 ± 32%	11 ± 12%
HA/(HA+PV)	-44 ± 15% *	-25 ± 18%	72 ± 38%

Values are shown as mean ± SEM (n = 10 pigs); HA, hepatic artery; PV, portal vein;

\*) Mean value was significantly different from zero (P<0.05).

**TABLE 3**

Relative error of DCE-CT estimated PV liver tissue blood perfusion using two versions of the slope method.

	Capnic Condition		
	Normocapnia	Hypocapnia	Hypercapnia
Subtraction Method	187 ± 63% *	238 ± 90% *	25 ± 46%
Direct Method	119 ± 67%	137 ± 104%	-39 ± 24%

Values are shown as mean ± SEM (n = 4);

\*) Mean value significantly different from zero (P&lt;0.05).